WCP2023
2 - 7 JULY 2023
GLASGOW | SCOTLAND

19TH WORLD CONGRESS OF BASIC AND CLINICAL PHARMACOLOGY

Register now

You could save nearly 40%*

*Early bird deadline: 17 March 2023

wcp2023.org

BRITISH PHARMACOLOGICAL SOCIETY

IUPHAR
INTERNATIONAL UNION OF BASIC AND CLINICAL PHARMACOLOGY

Visit Scotland | Alba
Business Events

GLASGOW CONVENTION BUREAU

Molecular mechanisms of MrgprA3-independent activation of the transient receptor potential ion channels TRPA1 and TRPV1 by chloroquine

Running Title: Activation of TRPA1 and TRPV1 by chloroquine

Tabea C. Fricke[1], Sebastian Pantke[1], Bjarne Lüttmann[1], Frank G. Echtermeyer[1], Christine Herzog[1], Mirjam J. Eberhardt[1], Andreas Leffler[1#]

1. Department of Anesthesiology and Intensive Care Medicine, Hannover Medical School, 30625 Hannover, Germany.

#Corresponding author:

Prof. Dr. med. Andreas Leffler

Department of Anesthesiology and Intensive Care Medicine

Hannover Medical School

Carl-Neuberg Strasse 1

30625 Hannover, Germany

Telephone: +49 511 532 8494

Email: leffler.andreas@mh-hannover.de

Bullet point summary

'What is already known'

- Chloroquine induces histamine-independent but MrgprA3-dependent itch

- Activation of MrgprA3 by chloroquine was suggested induce activation of TRPA1

'What this study adds'

- Chloroquine combined with UVA-light activate TRPA1 and TRPV1 by producing intracellular ROS.

- Chloroquine can activate TRPA1 and TRPV1 by inducing intracellular alkalization

' Clinical significance'.

- Chloroquine-induced itch and retinopathy patients might involve UVA-light and depend on oxidative stress

Abstract

Background and purpose: Itch associates several pathologies and is a common drug-induced side effect. Chloroquine (CQ) was reported to induce itch by activating the Mas-related G protein-coupled receptor MrgprA3 and subsequently TRPA1. In this study we demonstrate that CQ employs at least two MrgprA3-independent mechanisms to activate or sensitize TRPA1 and TRPV1.

Experimental Approach: Patch Clamp and calcium-imaging were utilized to examine effects of CQ on TRPA1 and TRPV1 expressed in HEK-293T cells.

Key Results: In calcium-imaging, CQ induces a concentration-dependent but MrgprA3-independent activation of TRPA1 and TRPV1. While CQ itself inhibits TRPA1 and TRPV1 in patch clamp recordings, co-application of CQ and UVA-light evokes membrane currents through both channels. This effect is inhibited by the reducing agent dithiothreitol (DTT) and reduced on mutants lacking cysteine residues accounting for reactive oxygen species (ROS)-sensitivity. The combination of CQ and UVA-light triggers an accumulation of intracellular ROS, removes fast inactivation of voltage-gated sodium currents and activates TRPV2. On the other hand, CQ is a weak base and induces intracellular alkalosis. Intracellular alkalosis can activate TRPA1 and TRPV1, and CQ applied at alkaline pH-values indeed activates both channels.

Conclusion and Implications: Our data reveal novel pharmacological properties of CQ allowing activation of TRPA1 and TRPV1 via photosensitization as well as intracellular alkalosis. These findings add complexity to the commonly accepted dogma that CQ-induced itch is specifically mediated by MrgprA3 coupling to TRPA1.

Keywords: itch, sensory neuron, histamine, chloroquine, oxidative stress

Abbreviations

A96	A967079
AITC	Allyl isothiocyanate
BCECF	2′,7′-Bis(2-carboxyethyl)-5(6)-carboxy-fluorescein
BCTC	4-(3-Chloro-2-pyridinyl)-N-[4-(1,1-dimethylethyl)phenyl]-1-piperazinecarboxamide
Cap	Capsaicin

CHO	Chinese Hamster Ovary
CQ	Chloroquine
DCFH-DA	2,7-dichlorodihydroflorescein diacetate
DRG	Dorsal Root Ganglion
DTT	Dithiothreitol
HEK 293	Human Enbryonic Kidney 293
MrgprA3	Mas-related G protein-coupled receptor A3
PLC	Phospholipase C
ROS	Reactive Oxygen Species
RR	Ruthenium red
TRP	Transient Receptor Potential
UVA	Ultraviolet A

1. Introduction

The classical pathway leading to itch is initiated by a release of histamine by mast cells, and it is commonly assumed that a histamine-receptor mediated activation of TRPV1 expressed in sensory neurons is an important peripheral event leading to itch (Kittaka & Tominaga, 2017; Schmelz, 2021; Shim, Tak et al., 2007). There is accumulating evidence that itch can also be mediated by histamine-independent mechanisms which seems to account for itch observed as side effects of different pharmacologic treatments as well as during the course of several pathological conditions (Kittaka & Tominaga, 2017; Kremer, Feramisco et al., 2021). Histamine-

independent itch is typically non-responsive to standard antihistaminic pharmacological treatments, e.g. it is a demanding clinical problem with an unmet need for effective therapeutic options. Accordingly, pre-clinical models allowing mechanistic and molecular analyses of histamine-independent itch in rodents have been developed. Chloroquine (CQ) is a drug primarily used for treatment and prevention of malaria, but also for treatment of other disorders including rheumatic diseases (Mnyika & Kihamia, 1991; Taylor & White, 2004). Itch is a limiting side effect of CQ that seems to be mediated by histamine-independent mechanisms. Liu and colleagues demonstrated that CQ-induced scratching in mice depends on the Mas-related G protein-coupled receptor MrgprA3 and postulated that CQ is an MrgprA3-agonist (Liu, Tang et al., 2009). CQ induced a rapid calcium-influx in a small population of mouse DRG neurons, suggesting that MrgprA3 coupled to ionotropic receptors (Liu, Tang et al., 2009). Wilson et al., indeed observed a TRPA1-dependent CQ-induced calcium-influx in DRG neurons and found that CQ-induced itch in vivo requires TRPA1 (Wilson, Gerold et al., 2011). This CQ-induced activation of TRPA1 was explained by a MrgprA3-mediated activation of phospholipase C coupling to TRPA1 (Wilson, Gerold et al., 2011). Results from recent studies have questioned the notion that CQ-induced activation of sensory neurons is exclusively mediated by this MrgprA3-PLC-TRPA1 signaling pathway (Ru, Sun et al., 2017; Than, Li et al., 2013). Than and co-workers demonstrated that among all mouse DRG neurons responding to 1 mM CQ, only 43% expressed TRPA1 (Than, Li et al., 2013). In the remaining CQ-sensitive population, CQ-induced responses were inhibited by TRPC3-inhibitors. Furthermore, CQ induced a strong potentiation of capsaicin-induced responses (Than, Li et al., 2013). Another suggests that CQ-induced activation of C-fibers is independent of TRPA1, TRPV1 and TRPC3, CQ-induced itch-like behavior in vivo does not require TRPA1 (Ru, Sun et al.,

2017). On the other hand, CQ injected into the mouse paw was reported to evoke a TRPA1-dependent thermal hyperalgesia and mechanical allodynia (Tsagareli, Nozadze et al., 2020). When trying to align these studies, MrgprA3 seems to be required for CQ-induced itch-related behavior, but it remains uncertain which mechanisms really account for CQ-induced activation of sensory neurons. We hypothesized that a possible reason for these ambiguities may be that different properties of CQ are likely to induce a yet unknown MrgprA3-independent activation of TRPA1 and/or TRPV1: 1. CQ induces oxidative stress and may even induce phototoxicity (Zhou, Chen et al., 2017). If so, CQ should gate ROS-sensitive ion channels like TRPA1 and TRPV1. 2. CQ is a weak base with a pKa of around 10.4. When applied at high concentrations, CQ may induce an intracellular alkalosis known to activate TRPA1 and TRPV1 (Dhaka, Uzzell et al., 2009; Fujita, Uchida et al., 2008). In the present study, we employed standard calcium-imaging and patch clamp techniques to examine if these properties enable CQ to directly modify or activate TRPA1 and TRPV1.

2. Materials & Methods

2.1. Chemicals

Chemicals were dissolved and purchased as follows: Chloroquine and hydroxychloroquine (both 100 mM in external solution), Dithiothreitol (DTT) (100 mM stock in external solution), Ruthenium red (RR) (10 mM stock in external solution), 2,7-

dichlorodihydroflorescein diacetate (DCFH-DA) (1 mM stock solved in DMSO) and 2′,7′-Bis(2-carboxyethyl)-5(6)-carboxy-fluorescein (BCECF) were purchased from Sigma-Aldrich (Taufkirchen, Germany). A967079 and 4-(3-Chloro-2-pyridinyl)-N-[4-(1,1-dimethylethyl)phenyl]-1-piperazinecarboxamide (BCTC) were obtained from Tocris (Bio-Technology, Wiesbaden-Nordstadt, Germany).

2.2. Cell Culture

HEK 293T, CHO and ND7/23 cells were cultured under standard cell culture conditions (5% CO_2 at 37°C) in Dulbecco's modified Eagle's medium nutrient mixture F12 (DMEM/F12 Gibco/Invitrogen, Darmstadt, Germany) supplemented with 10% fetal bovine serum (Biochrom, Berlin, Germany). Using jetPEI (VWR, Darmstadt, Germany), cells were transfected with different plasmids for hTRPA1 wildtype, mTRPA1, hTRPA1-C621S/C641S/C665S, rTRPV2 wildtype, rTRPV2-M528I/M607I, MrgprA3 and hTRPV1 wildtype. Cells were detached after 24h of transfection using phosphate buffered saline (PBS, Lonza, Cologne, Germany) and seeded for patch clamp or calcium-imaging experiments. cDNA of MrgprA3 was a kind gift from Dr. Xinzhong Dong (Baltimore, U.S.A). HEK 293 cells with a stable expression of TRPA1 and TRPV1 were cultured and used as previously described (Palmaers et al., 2021). CHO cells with a stable expression of mTRPA1 were kindly provided by Dr. Ardem Patapoutian (San Diego, U.S.A.).

DRG neurons from C57Bl/6 wildtype, was performed as described previously (Palmaers, Wiegand et al., 2021). Mice were anaesthetized by isoflurane and sacrificed by decapitation. DRGs from all levels were excised and transferred to Dulbecco's modified Eagle's medium (DMEM). DRGs were treated with DMEM containing 1 mg/ml collagenase and 0.5 mg/mL protease for 45 min (both from Sigma-

Aldrich, Taufkirchen, Germany) and then dissociated using a fire-polished, silicone-coated Pasteur pipette. Isolated cells were transferred onto poly-L-lysine-coated (0.1 mg/mL, Sigma Aldrich) coverslips and cultured in TNB 100 medium supplemented with TNB 100 lipid protein complex, penicillin/streptomycin (100 U/mL) (all from Biochrom, Berlin, Germany). Cells were used for experiments within 24 h after plating. All procedures of this study were approved by the animal protection authorities (local district government, Hannover, Germany).

2.3. Patch Clamp

Recordings were performed at room temperature using an EPC10 USB amplifier (HEKA Elektronik, Lamprecht, Germany). Signals were low passed at 1 kHz and sampled at 2 to 10 kHz. During whole-cell measurements cells were held at -60 mV, during inside- out and on cell voltage recordings at +60 mV. Pipettes were pulled from borosilicate glass tubes (TW150F-3; World Precision Instrument, Berlin, Germany) to give a resistance of 2.0– 5.0 MΩ and filled with the standard pipette solution containing (in mM): KCl 140, MgCl$_2$ 2, EGTA 5 and HEPES 10 (pH 7.4 was adjusted with KOH). The standard external solution contained (in mM): NaCl 140, KCl 5, MgCl$_2$ 2, EGTA 5, HEPES 10 and glucose 10 (pH 7.4 was adjusted with NaOH). All experiments were performed at room temperature. The Patchmaster software (HEKA Elektronik) was used to apply heat ramps as described previously (Fricke et al., 2019). Briefly, the current is passed to an insulated copper wire coiled around the capillary tip of the common outlet of the perfusion system. This heats the solutions from room temperature to about 45°C within 5s. A miniature thermocouple is fixed at the orifice of the capillary tip to measure the temperature of the super fusing solution (Dittert, Benedikt, Vyklicky, Zimmermann, Reeh & Vlachova, 2006). A gravity-driven multi-

barrel perfusion system was used to apply solutions. Patchmaster/Fitmaster software (HEKA Elektronik) and Origin 8.5.1 (Origin Lab, Northampton, MA, U.S.A) were used to perform off-line analysis and data acquisition. A combination of the light source (HXP 120, LEJ lightning & electronics Jena, Germany) and a filter set consisting of a 340 nm and 380 nm exciter and 400 nm dichroic long pass filter (Chroma ET 79001, Chroma Technology GmbH, Olching, Germany) was used for illumination of cells and substances. For all patch clamp experiments, experiments were not randomly assigned, and the experimenters were not blinded to the experiment.

2.4 Ratiometric $[Ca^{2+}]_i$ and pH measurements

Cells were seeded on coverslips 24h prior to measurements and stained for 45 minutes with 0.02% pluronic and 4 µM Fura-2-AM or 4µM BCECF-AM. After the subsequent wash out, cells were mounted on an inverse microscope (Axio observer D1; Zeiss, Jena, Germany). Fura-2 was excited at 340 and 380 nm and BCECF at 500 and 436nm using a light source (HXP 120, LEJ lightning & electronics Jena, Germany), LEP filter wheel (Ludl electronic products Ltd., Hawthorne, New York) and appropriate filter sets (Chroma Technology GmbH, Olching, Germany). With a CCD camera (Cool SNAP EZ; Photometrics, Puchheim, Germany) images were acquired at 1 Hz and exposed for respectively 10 and 20 ms for calcium-imaging and 5ms for imaging using BCECF. Data were recorded with VisiView 2.1.1 software (Visitron Systems GmbH, Puchheim, Germany). Standard imaging solution (pH 7.4) contained (in mM) NaCl 145, KCl 5, $CaCl_2$, 1.25, $MgCl_2$ 1, glucose 10 and HEPES 10. Before calculation of the ratios, background fluorescence was subtracted. Functional expression of TRPA1 and TRPV1 was verified with carvacrol and capsaicin respectively. Results are presented as mean (± S.E.M.) of the ratio F340/380 nm for

calcium-imaging and ratio F500/436 nm for BCECF-imaging). In all calcium-imaging experiments, experiments were not randomly assigned. However, the experimenter was blinded to the background and purpose of the experiment, e.g. the person was only informed about the experimental protocols.

2.5. ROS Assay on ND7/23 Cells

The fluorescent marker DCFH-DA was used for the measurements of intracellular ROS according to the manufacturer's instructions. ND7/23 cells were seeded in 12 - well plates 24 h before treatment and washed with phosphate buffer saline (PBS) before the medium was renewed and 300 μM CQ alone or with 10 mM DTT were added. After 10 min UVA-irradiation, 5 μM DCFH-DA dye was added to the medium and the cells were incubated for 30 min under standard cell culture conditions. Subsequently, cells were washed and five randomly selected high power fields were documented with 10x magnification on an inverted fluorescence microscope (IX81; Olympus, Tokyo, Japan). The DCFH-DA-stained area was analyzed with ImageJ Software (National Institutes of Health, Bethesda, MD, U.S.A.). The ROS assay experiments were not randomly assigned. The experimenter was blinded to the background and purpose of the experiment, e.g. the person was only informed about the experimental protocols.

2.6. Statistical analyses

All data are represented as mean ± S.E.M. For data representing calcium-imaging experiments, the given n-number represent the total recorded number of cells. These data were collected in >5 separate experiments and data were collected on 1- 3 experimental days for each data set. Calcium-imaging data were not used for

statistical analyses. For data representing patch clamp experiments, the given n-number represent the total recorded number of included cells usually recorded on 1-2 experimental days. Patch Clamp data for statistical comparisons were not normally distributed (Shapiro-Wilk Test). Comparisons between two groups with small sample sizes (n ≥ 5) were performed by non-parametric testing using the Mann-Whitney U-test for unpaired data. The Kruskal Wallis Test was used for comparisons of >2 groups. Statistical analysis was performed using GraphPad Prism 5 or 9 (GraphPad Software Inc., La Jolla, U.S.A.). Significance was assumed for p< 0.05. * denotes p< 0.05, ** p< 0.01, *** p< 0.001. The authors of this study followed the recommendations set out in editorials of British Journal of Pharmacology where appropriate.

3. Results

Chloroquine activates TRPA1

Human TRPA1 (hTRPA1) stably expressed in HEK 293 cells was examined by ratiometric calcium-imaging (Supplement Figure 1A and B). Increasing concentrations of CQ (30, 100, 300 and 1000 µM) applied in separate experiments were applied for 120 s each. Only 1 mM CQ induced an instant increase in intracellular calcium that declined over time (Fig. 1A). However, we observed a concentration-dependent increase in intracellular calcium following washout of CQ (Fig. 1A and Supplement Figure 1C- F, n> 200 cells for each concentration). In non-transfected cells, 1 mM but not 300 µM CQ also evoked a small but robust increase in intracellular calcium, e.g. this effect does not seem to be solely mediated by hTRPA1 (Fig. 1B, n= 282 and 461 respectively, Supplement Figure 1G). However, non-transfected cells failed to produce

calcium-influx following washout of both 300 µM and 1 mM CQ (Fig. 1B). Considering that 1 mM CQ seems to induce a TRPA1-independent calcium increase in HEK 293T cells, further calcium-imaging experiments were performed with 300 µM CQ. To confirm that the "late" CQ-induced increase in intracellular calcium seems to be mediated by hTRPA1, we performed experiments with 300 µM CQ co-applied with 10 µM of the selective TRPA1-inhibitor A967079. Indeed, cells treated with A967079 and 300 µM CQ failed to produce a prominent increase in intracellular calcium following wash out of CQ (Fig. 1C, n= 546, Supplement Figure 1H). These data indicate that CQ activates hTRPA1 in HEK 293T cells which had not been transfected with MrgprA3. To substantiate these somewhat intriguing findings obtained with ratiometric calcium-imaging experiments only able to detect an elevation of intracellular calcium, we utilized whole-cell patch clamp to examine if CQ indeed induces membrane currents through hTRPA1. To our surprise, CQ at any concentration failed to induce membrane currents in these cells. Instead, CQ induced a concentration-dependent inhibition of outward currents observed during 500 ms long voltage ramps reaching from -100 mV to +100 mV in the cells (Fig. 1D, n= 6). Thus, there was a striking difference between data obtained by calcium-imaging and patch clamp. An evident difference between these two methods is the illumination of cells with UVA-light when performing calcium-imaging. Therefore, we performed further patch recordings in which cells treated with 1 mM CQ were exposed to the same UVA-light source used for calcium-imaging. As is demonstrated in figure 1E, this combined application of CQ and UVA-light indeed resulted in large membrane currents. Of note, these currents strongly increased once CQ was washed out (n= 8). In non-transfected cells, application of 1 mM CQ and UVA-light did not induce membrane currents above baseline (Fig. 1F, n= 6). When cells were constantly held at -60 mV, neither UVA-light

nor CQ alone evoked inward currents in cells expressing hTRPA1 (Fig. 1G). However, the combination of CQ and UVA-light evoked prominent inward currents. Again, washout of CQ resulted in a rapid increase in current amplitude that was reduced by a repeated application of CQ. These CQ + UVA-light-induced currents were effectively inhibited by A967079 (Fig. 1G and H, n= 10). These CQ + UVA-light induced effects were not observed in non-transfected cells (Supplement Figure 2A). In order to substantiate our interpretation that CQ also inhibits hTRPA1, we examined the effect of 1 mM CQ on inward currents evoked by 100 µM allyl isothiocyanate (AITC). Indeed, CQ induced a partial and reversible inhibition of these currents (Supplement Figure 2B, 61 ± 8% inhibition, n= 8). The combined application of CQ and UVA-light also evoked A967079-sensitive membrane currents in both cell-attached (Fig. 1I, n= 8) and cell-free inside-out recordings (Fig. 1J, n= 5). These data suggest that CQ + UVA-light, but not CQ alone induce gating of TRPA1 through a mechanism independent from cytosolic factors. The chloroquine-derivative hydroxychloroquine induced similar, but smaller effects on hTRPA1 when co-applied with UVA-light (Supplement Fig. 2C and D).

MrgprA3 does not seem to increase CQ-induced activation of TRPA1

Previous reports found that MrgprA3 mediates CQ-induced calcium-influx in HEK 293 cells lacking recombinant expression of TRP channels (Liu, Tang et al., 2009), and that activation of MrgprA3 by CQ results in an activation of TRPA1 (Wilson, Gerold et al., 2011). As our data suggest that CQ can induce effects in cells lacking MrgprA3, we asked if we can determine an effect of MrgprA3 for CQ-induced calcium-influx or inward currents in our experimental conditions. First, we explored if transient expression of MrgprA3 in HEK 293T cells results in an increased response to 1 mM

CQ. As is demonstrated in figure 2A (and Supplement Figure 3A) however, MrgprA3 did not seem to alter the small CQ-induced effect in HEK 293T cells (n= 889). Next, the role of MrgprA3 for activation of hTRPA1 by 300 µM CQ was examined (Fig. 2B-D). CQ induced similar responses in cells expressing only hTRPA1 (Fig. 2C, n= 54) as in cells co-expressing hTRPA1 and MrgprA3 (Fig. 2D, n= 370). However, cells expressing MrgprA3 + hTRPA1 seemed to generate a somewhat faster CQ-induced calcium-influx than cells expressing only hTRPA1. This difference is obvious both for the average responses of all cells (Fig. 2B) as well as for original traces from single cells (Fig. 2C and D). This effect was not observed in patch clamp recordings, e.g. MrgprA3-expressing cells displayed even slightly smaller CQ + UVA-light-induced inward currents as compared to cells expressing only hTRPA1 (Fig. 2E and F, n= 7, p< 0.05 Mann-Whitney-U-Test). A possible reason for our failure to identify a MrgprA3-dependent effect this is that mouse MrgprA3 might not couple to human TRPA1. Therefore, we aimed to conduct experiments in cells co-expressing mouse (m) TRPA1 and MrgprA3. In our hands, transient expression of mTRPA1 in HEK 293T cells results in cells with a very poor viability and high basal intracellular calcium levels. Therefore, we explored mTRPA1 expressed in chinese hamster ovary (CHO) cells. Expression of mTRPA1 in CHO-cells indeed resulted in a "late" CQ-induced calcium-influx becoming evident following washout of 1 mM CQ (n= 296 and 476 respectively, Fig. 2G, Supplement Figure 3B and C). While the CHO cells expressing mTRPA1 already displayed relatively high basal calcium levels, our attempts to establish a co-expression of mTRPA1 and MrgprA3 in CHO cells resulted in very high calcium levels unsuitable for calcium-imaging experiments. Nevertheless, we were able to perform whole-cell patch clamp recordings on CHO cells expressing mTRPA1 without or with MrgprA3. When 1 mM CQ was applied without UVA-light, minimal inward currents

were induced in cells expressing mTRPA1 + MrgprA3 (Fig. 2H, n= 9). Similar to hTRPA1 expressed in HEK 293T cells however, mTRPA1 expressed without MrgprA3 in CHO cells produced robust inward currents when challenged with CQ and UVA-light (Fig. 2I, n= 8). Taken together, we were not able to define the role of MrgprA3 for activation of hTRPA1 and mTRPA1 by CQ + UVA-light in our experiments.

CQ-induced calcium-influx in neuroblastoma ND7/23 cells and mouse DRG neurons

Our data obtained in HEK 293T and CHO cells demonstrate that the combined application of CQ and UVA-light can activate both human and mouse TRPA1. We next asked if this effect can be observed in neuronal cells as well. ND7/23 cells are hybrid cells generated by mouse neuroblastoma and rat DRG neurons. As is demonstrated in figure 3A, ND7/23 cells with a transient expression of hTRPA1 displayed the typical "late" increase in intracellular calcium following application of 1 mM CQ (n= 373). However, non-transfected ND7/23 cells almost completely failed to respond to CQ (Fig. 3A, n= 354). When observing representative experiments from individual cells, responses of ND7/23 cells with hTRPA1 displayed a uniform shape, e.g. with a "late" response occurring after washout of CQ (Fig. 3B). Next, the effect of 1 mM CQ was examined on mouse DRG neurons. In contrast to ND7/23 cells, we observed a very heterogenous response pattern with immediate fast as well as late responses when observing original traces from individual DRG neurons (Fig. 3C). We compared the responses to 1 mM CQ between all recorded neurons (n= 459), AITC-sensitive (n= 139, e.g. TRPA1-positive) and AITC-negative (n= 320, e.g. TRPA1-negative) neurons (Fig. 3D). While neurons lacking TRPA1 displayed no or very small responses to CQ, the TRPA1-expressing cells indeed seemed to define a "highly CQ-sensitive"

population. A similar, but not as evident separation between CQ-sensitive and CQ-insensitive DRG neurons was achieved by comparing capsaicin-sensitive (n= 236) and capsaicin-insensitive neurons (n= 223) (Fig 3E). These data suggest that CQ-sensitivity is high in the population of DRG neurons expressing TRPV1 and TRPA1. In order to investigate if TRPA1 or TRPV1 are generating CQ-induced calcium-influx in these cells, we conducted experiments with 1 mM CQ application together with either the TRPA1-antagonist A967079 (n= 216) or the TRPV1-antagonist BCTC (n= 88). However, CQ-induced calcium-influx were not markedly reduced by block of either TRPA1 or TRPV1 (Supplement 4). Therefore, we performed a final experiment with co-application of CQ, A967079 and BCTC (n= 56). Indeed, the combined inhibition of both TRPA1 and TRPV1 almost fully inhibited CQ-induced calcium-influx (Fig. 3F).

Co-application of CQ and UVA-light induces a sustained activation of ROS-sensitive TRP channels.

We now aimed to learn how CQ + UVA-light activate TRPA1. When illuminated with UVA-light, photosensitizers produce reactive oxygen species (ROS) that activate redox-sensitive TRP channels like TRPA1, TRPV1 and TRPV2 (Babes, Sauer et al., 2016; Fricke, Echtermeyer et al., 2019). CQ was reported to induce and an elevation of ROS in ND7/23 cells when added to the culture media (Zhou, Cheng et al., 2017). We therefore asked if CQ might give rise to intracellular ROS when illuminated with UVA-light. We first examined if the reducing agent DTT inhibits CQ + UVA-light induced activation of hTRPA1. Indeed, application of 10 mM DTT with 1 mM CQ resulted in a reduced response as compared to the effect induced by CQ applied alone (Fig. 4A, n= 465, Supplement Figure 5A). Simultaneous application of 10 mM DTT with 1 mM CQ + UVA-light also resulted in a significant reduction of the amplitudes of

inward currents (Fig. 4B and C, n= 7, p< 0.001, Mann-Whitney-U-Test). Furthermore, inward currents induced by CQ and UVA-light were partially reversed by 10 mM DTT (80 ± 2%, Fig. 4D, n= 6). We next examined a hTRPA1-mutant lacking intracellular cysteine residues being important for ROS-sensitivity (hTRPA1-C621S/C641S/C665S, hTRPA1-3C). As is demonstrated in figure 4E, hTRPA1-3C produced a small but still prominent calcium-influx when challenged with 300 µM CQ (n= 200, Supplement Figure 5B). Patch clamp recordings on hTRPA1-3C also showed a reduction of the current amplitudes as compared to hTRPA1-WT (Fig. 4F and G, n= 8, p< 0.01, Mann-Whitney-U-Test).

We and others have previously demonstrated that TRPV1 can be activated by photosensitizing agents by means of ROS-sensitivity as well (Babes, Sauer et al., 2016; Fricke, Echtermeyer et al., 2019). In order to examine the effect of CQ and UVA-light on human (h)TRPV1, we employed stably expressing HEK 293-hTRPV1 cells (Supplement Figure 6A, B, n= 699). Indeed, calcium-imaging experiments on these cells revealed a concentration-dependent (100, 300 and 1000 µM) increase in intracellular calcium (Fig. 5A, n >250 for each concentration, Supplement Figure 6C-E). When compared to hTRPA1, hTRPV1 seems to be less CQ-sensitive and produced robust responses only with 1 mM CQ. In contrast to TRPA1, washout of CQ did not result in a prominent increase, but rather in a sustained elevation of intracellular calcium in hTRPV1-expressing cells. The simultaneous application of CQ with the TRPV1-inhibitor BCTC (100 nM) almost fully inhibited CQ-induced increase in intracellular calcium (Fig. 6B, n= 117, Supplement Figure 6F). In whole-cell patch clamp recordings, voltage-ramps reaching from -100 to +100 mV displayed a concentration-dependent (30, 100, 300 and 1000 µM) inhibition of outward currents (Fig. 6C, n= 5). As is shown in figure 5D, concurrent illumination with UVA-light during

application of CQ evoked a small membrane current that increased following washout of CQ. In cells held at -60 mV, application of CQ and UVA-light induced a small inward current that increased following washout of CQ and was inhibited by BCTC (Fig. 5E and F, n= 6). Cell-free inside-out recordings showed that CQ and UVA-light seem to directly gate hTRPV1 (Fig. 5G, n= 6). In order to examine if CQ is able to sensitize hTRPV1, heat-evoked inward currents were studied. As is demonstrated in figure 5H and I, even 1 mM CQ itself induced a modest potentiation of heat-evoked currents. This effect could be further increased by UVA-light, and again there was a large increase in current amplitude following washout of CQ (n= 7).

We recently demonstrated that TRPV2 displays a methionine-dependent ROS-sensitivity (Fricke, Echtermeyer et al., 2019). Therefore, the effects of CQ on rat TRPV2 (rTRPV2) were explored. Similar to TRPA1 and TRPV1, cells expressing rTRPV2 generated membrane currents following treatment with CQ and UVA-light (Fig. 6A, n= 8). The combination of 1 mM CQ and UVA-light also induced large heat-evoked currents through rTRPV2 (Fig. 6B and C, n= 10). 2-APB-evoked inward currents were strongly potentiated by 1 mM CQ applied together with UVA-light (Fig. 6D, n= 10). This effect was reduced on the ROS-insensitive mutant rTRPV2-M528I/M607I (Fig. 6E and F, n= 8, p= 0.153, p< 0.05, p< 0.01, Kruskal Wallis Test). Taken together, these data indicate that CQ can activate ROS-sensitive TRP channels when illuminated with UVA-light.

In order to further corroborate our interpretation that CQ and UVA-light induce oxidative stress, we next asked if the combination of CQ + UVA-light can mimic the action of strong oxidants such that they remove fast inactivation of voltage-gated sodium channels (Kassmann, Hansel et al., 2008). As is demonstrated in figure 7A, application of CQ alone induced a concentration-dependent block of sodium currents

in ND7/23 cells (n= 9). When challenging cells with UVA-light, we observed a small reduction of fast inactivation (Fig. 7B, n= 9). When 100 µM CQ was co-applied with UVA-light however, we observed a stronger loss of fast inactivation over time (Fig. 7C, D; n= 9). We also used ND7/23 cells for a H2DCFDA-based ROS-assay to visualize an accumulation of intracellular ROS following treatment with CQ and UVA-light. As is demonstrated figure 7E- H, cells treated with CQ and UVA-light displayed high ROS-levels. This increase in ROS was reduced when DTT was co-incubated with CQ and UVA-light (Fig. 7H). In support of these preliminary data showing elevated ROS-levels following treatment with CQ and UVA-light, we feel it is justified to conclude that this is likely to be the main mechanism for activation of ROS-sensitive TRP channels by CQ and UVA-light.

Chloroquine-induced intracellular alkalization may contribute to a transient activation of TRPA1 and TRPV1.

CQ is a weak base with a pKs-value of 10.4, e.g. when applied at high concentrations it should induce intracellular alkalization. Considering that both TRPA1 and TRPV1 are activated by intracellular alkalosis (Dhaka, Uzzell et al., 2009; Fujita, Uchida et al., 2008), we explored if this property of CQ contributes to activation of any of these channels. First, imaging experiments with the fluorescent pH-indicator BCECF were performed on untransfected HEK 293T cells (n= 754) as well as on hTRPA1-expressing (n= 537) cells. During application of 1 mM CQ, the fluorescence signal increased in both cell types. However, cells expressing hTRPA1 displayed a stronger signal (Fig. 8A). This result confirms that CQ can induce intracellular alkalosis, and that expression or even activation of TRPA1 may enhance this effect. Considering that extracellular alkalization increases the fraction of uncharged und thus membrane-

permeable CQ molecules, we investigated if alkalosis potentiates activation of hTRPA1 by CQ. Calcium-imaging experiments were performed on hTRPA1-expressing cells treated with 300 µM CQ at pH 7.4, 300 µM CQ at pH 8.4 or with control solution at pH 8.4. As is demonstrated in figure 8B, application of control solution at pH 8.4 evoked a small and reversible increase in intracellular calcium (n= 883, Supplement Figure 7A). When CQ was applied at pH 8.4 however, cells generated a large and instant increase in intracellular calcium which was followed by a sustained effect after washout of CQ (Fig. 8B, n= 947, Supplement Figure 7B). In patch clamp experiments on cells expressing hTRPA1, application of control solution at pH 9 evoked a small and reversible inward current (Fig. 8C). When 1 mM CQ was applied at pH 9 however, we observed larger inward currents that were followed by a prominent and partly sustained current increase following washout of CQ (Fig. 8C and D, n= 12). While the standard external solution containing 10 mM HEPES was set at pH 7.4, the addition of 1 mM CQ elevated the pH-value to 7.7. When reducing HEPES to only 100 µM, 1 mM CQ elevated the pH-value to 8.2. When this CQ-containing solution was applied on hTRPA1, it induced small, rapidly activating and reversible inward currents (Fig. 8E, n= 8).

We also examined if hTRPV1 displays this pH-dependent activation by CQ. As is demonstrated in figure 9A, control solution titrated to pH 8.4 did not induce an obvious calcium-influx in cells expressing hTRPV1. When 300 µM CQ was applied at pH 8.4 however, hTRPV1-expressing cells generated a reversible increase in intracellular calcium. (Fig. 9A, n= 495 resp. 667, Supplement Figure 7C and D). Whole-cell patch clamp recordings revealed that at pH 9 - which by itself induced small inward currents - the addition of 1 mM CQ evoked large inward currents showing a fast increase in amplitude following washout (Fig. 9B and C, n= 7). In contrast to hTRPA1, hTRPV1

was not activated by 1 mM CQ in the solution containing 100 µM HEPES. However, using the reduced HEPES concentration (100 µM), 1 mM CQ induced a potentiation of heat-induced currents (Fig. 9D and E, n= 8).

4. Discussion

In this study we present novel and maybe rather unexpected data showing that CQ activates the polymodal ion channels TRPA1 and TRPV1 by at least two distinct MrgprA3-independent mechanisms. CQ seems to induce an intracellular accumulation of ROS upon illumination with UVA-light, e.g. a property typical for photosensitizing substances. Accordingly, co-application of CQ and UVA-light evokes sensitization or activation of the ROS-sensitive ion channels TRPA1, TRPV1, TRPV2. It also impairs fast inactivation of voltage-gated sodium channels, an effect which is known to require rather strong oxidation by intracellular methionine residues (Kassmann, Hansel et al., 2008). While this property may be of limited relevance when CQ is used to evoke acute itch-related behavior in rodents, it should be taken into account for in vitro experiments. Furthermore, it may be relevant for itch described as a side effect when CQ is used for prophylaxis or therapy of malaria. On the other hand, CQ is a weak base and we demonstrate that it permeates the cell membrane to induce an intracellular alkalosis. Our data indicate that high concentrations of CQ applied at alkaline pH-values sensitize or activate both TRPA1 and TRPV1 of which both are gated by intracellular alkalosis (Fujita, Uchida et al, 2008; Dhaka, Uzzell et al, 2009). Considering that the commonly performed in vivo model for CQ-induced itch in rodents foresees a subcutaneous injection of 40 mM CQ, it might very well be that a transient intracellular alkalosis might contribute to pain- or itch-related behavior by activating TRPA1 and TRPV1. Taken together, both properties of CQ identified in this study should be taken

into consideration when high concentrations of CQ are used for models of histamine-independent itch.

In the past decade, a large number of groundbreaking studies on molecular mechanisms mediating itch has been published and our understanding of how different pruritogens can activate peripheral sensory neurons includes a myriad of mechanisms (Kittaka & Tominaga, 2017; Schmelz, 2021). There is meanwhile little doubt about that several members of the Mas-related G protein-coupled receptor (Mrgpr) family serve as important itch-receptors in both rodents and humans (Liu & Dong, 2015). MrgprA3 is supposed to mediate histamine-independent itch in rodents, and an elegant study from Han and co-workers even suggested that the population of MrgprA3-expressing sensory neurons is a "labelled-line" for itch that exclusively innervates the epidermis (Han, Ma et al., 2013). More recent studies found that MrgprA3 is expressed in rather large subsets of sensory neurons innervating visceral organs such as the bladder and colon (Castro, Harrington et al., 2019; Grundy, Caldwell et al., 2021). To our knowledge, CQ is the only known substance which is considered to activate MrgprA3. The initial finding from Liu and colleagues presented strong evidence that CQ-induced activation of sensory neurons requires MrgprA3, and they suggested that CQ is likely to be an MrgprA3-agonist (Liu, Tang et al., 2009). This conclusion was drawn based on the finding that CQ induces an increase in intracellular calcium in HEK 293 cells expressing MrgprA3 (Liu, Tang et al., 2009). Thus, it is not clear if CQ indeed directly interacts with MrgprA3. Even more puzzling is the notion that expression of MrgprA3 enabled HEK 293 cells to generate a CQ-induced calcium-influx. MrgprA3 is a "non-ionotropic" G-protein coupled receptor, e.g. it is evident that calcium-influx is not directly driven by MrgprA3. Wilson and colleagues did not observe

a CQ-induced effect in HEK 293 expressing only MrgprA3, but suggested that CQ-induced calcium-influx requires expression of TRPA1 and is specifically mediated by a MrgprA3-PLC signaling cascade (Wilson, Gerold et al., 2011). Our data on MrgprA3 does not allow us to put previous studies into question, but we can conclude that expression of MrgprA3 did not play a major role for CQ-induced activation of TRPA1 in our experimental settings. As both previous studies employed mainly FURA2-based calcium-imaging to study effects of CQ (Liu, Tang et al., 2009; Wilson, Gerold et al., 2011), it is possible that the properties of CQ identified in the present study – e.g. e intracellular ROS and alkalosis – might have been playing a relevant role in these studies as well. The study from Wilson et al., found that TRPA1 is crucial for CQ-induced calcium-influx in DRG neurons and for itch (Wilson, Gerold et al., 2011). Although later studies have identified several further mechanisms which seem to be relevant for CQ-induced itch as well, it is not surprising that the deletion of TRPA1 results in a strongly reduced calcium signal upon application of a photosensitizer and/or a weak base. For both these insults, TRPA1 is the most prominent detector in cultured DRG neurons (Babes, Sauer et al., 2016; Fujita, Uchida et al., 2008). Furthermore, TRPA1 also seems to be required for itch-related behavior evoked by oxidative stress (Liu & Ji, 2012). For some reason, Wilson and co-authors did not detect the CQ-induced activation and sensitization of TRPV1 observed in the present study as well as by Than and co-workers (Than, Li et al., 2013). Than et al., reported that CQ-induced sensitization of TRPV1 requires MrgprA3, but our data clearly demonstrate that CQ can activate TRPV1 both via oxidation and intracellular alkalosis (Than, Li et al., 2013). Given that sensory neurons express a large number of at least ROS-sensitive proteins, it is likely that CQ-induced itch results from a modulation of several transduction molecules in sensory neurons. This notion is not only supported

by our data in mouse DRG neurons, but also by recent studies failing to demonstrate an important role of TRPA1 for CQ-induced activation of sensory neurons and for itch-related behavior(Than, Li et al., 2013, Ru, Sun et al., 2017). The present study even suggests that MrgprA3 is not required for CQ-induced activation of TRPA1 and TRPV1, and this finding raises the question how MrgprA3 mediates CQ-induced itch. In order to address this question, the molecular pharmacology of MrgprA3 needs to be studied in more detail. Besides from the fact that CQ is used as a model substance to study mechanisms mediating histamine-independent itch, intake of CQ for treatment of malaria and other disorders seems to be associated with itch (Mnyika & Kihamia, 1991). While the relevance of CQ-induced activation of sensory neurons due to intracellular alkalosis is likely to be limited to rather artificial in vitro and in vivo experiments where CQ is applied at high (millimolar) concentrations, it is tempting to speculate about a possible clinical relevance of the photosensitizing effect of CQ identified in this study. Thus, similar to several other known therapeutics with photosensitizing properties, accumulation of CQ in the epidermis may result in a phototoxic reaction following illumination with UV-light (e.g. sun light). While there is only vague evidence for a clinically relevant phototoxicity of CQ (Callaly, FitzGerald et al., 2008; Motten, Martinez et al., 1999), Zhou et al. demonstrated that antioxidant treatment inhibited CQ-induced itch-related behavior in vivo (Zhou, Cheng et al., 2017). They also found that CQ induces an accumulation of intracellular ROS in cells in vitro. We could not only confirm this effect, but we also demonstrate that UVA-light can strongly potentiate CQ-induced oxidative stress. Taking this issue further, it is possible that the property of CQ to act as a photosensitizer may also be relevant for CQ-induced retinopathy (Glickman, 2002). CQ seems to accumulate in choroidal melanocytes, and ROS-sensitive TRP channels like TRPA1 and TRPV1 are

expressed in retinal pigment epithelia and in melanocytes (Eves, Smith-Thomas et al., 1999). Whether or not retinopathy is a result of an UV-light-induced increased oxidative stress and cell injury in presence of CQ, needs to be further explored.

5. Conclusions

The data presented in this study – at least in part – refute the current understanding how CQ activates sensory neurons, e.g. that CQ activates MrgprA3 which couples to TRPA1 via PLC. Our data do not show that this signaling pathway is not relevant for CQ-induced itch, but we do demonstrate that CQ activates TRPA1 and TRPV1 by inducing intracellular ROS and alkalosis. These two MrgprA3-independent mechanisms need to be taken into account when CQ is used to induce histamine-independent itch.

References

Babes A, Sauer SK, Moparthi L, Kichko TI, Neacsu C, Namer B*, et al.* (2016). Photosensitization in Porphyrias and Photodynamic Therapy Involves TRPA1 and TRPV1. J Neurosci 36**:** 5264-5278.

Callaly EL, FitzGerald O, & Rogers S (2008). Hydroxychloroquine-associated, photo-induced toxic epidermal necrolysis. Clin Exp Dermatol 33**:** 572-574.

Castro J, Harrington AM, Lieu T, Garcia-Caraballo S, Maddern J, Schober G*, et al.* (2019). Activation of pruritogenic TGR5, MrgprA3, and MrgprC11 on colon-innervating afferents induces visceral hypersensitivity. JCI Insight 4.

Dhaka A, Uzzell V, Dubin AE, Mathur J, Petrus M, Bandell M*, et al.* (2009). TRPV1 is activated by both acidic and basic pH. J Neurosci 29**:** 153-158.

Dittert I, Benedikt J, Vyklicky L, Zimmermann K, Reeh PW, & Vlachova V (2006). Improved superfusion technique for rapid cooling or heating of cultured cells under patch-clamp conditions. J Neurosci Methods 151**:** 178-185.

Eves P, Smith-Thomas L, Hedley S, Wagner M, Balafa C, & Mac Neil S (1999). A comparative study of the effect of pigment on drug toxicity in human choroidal melanocytes and retinal pigment epithelial cells. Pigment Cell Res 12**:** 22-35.

Fricke TC, Echtermeyer F, Zielke J, de la Roche J, Filipovic MR, Claverol S*, et al.* (2019). Oxidation of methionine residues activates the high-threshold heat-sensitive ion channel TRPV2. Proc Natl Acad Sci U S A 116**:** 24359-24365.

Fujita F, Uchida K, Moriyama T, Shima A, Shibasaki K, Inada H*, et al.* (2008). Intracellular alkalization causes pain sensation through activation of TRPA1 in mice. J Clin Invest 118**:** 4049-4057.

Glickman RD (2002). Phototoxicity to the retina: mechanisms of damage. Int J Toxicol 21**:** 473-490.

Grundy L, Caldwell A, Garcia-Caraballo S, Grundy D, Spencer NJ, Dong X*, et al.* (2021). Activation of MrgprA3 and MrgprC11 on Bladder-Innervating Afferents Induces Peripheral and Central Hypersensitivity to Bladder Distension. J Neurosci 41**:** 3900-3916.

Han L, Ma C, Liu Q, Weng HJ, Cui Y, Tang Z*, et al.* (2013). A subpopulation of nociceptors specifically linked to itch. Nat Neurosci 16**:** 174-182.

Kassmann M, Hansel A, Leipold E, Birkenbeil J, Lu SQ, Hoshi T*, et al.* (2008). Oxidation of multiple methionine residues impairs rapid sodium channel inactivation. Pflugers Arch 456**:** 1085-1095.

Kittaka H, & Tominaga M (2017). The molecular and cellular mechanisms of itch and the involvement of TRP channels in the peripheral sensory nervous system and skin. Allergol Int 66**:** 22-30.

Kremer AE, Feramisco J, Reeh PW, Beuers U, & Oude Elferink RP (2014). Receptors, cells and circuits involved in pruritus of systemic disorders. Biochim Biophys Acta 1842**:** 869-892.

Liu Q, & Dong X (2015). The role of the Mrgpr receptor family in itch. Handb Exp Pharmacol 226**:** 71-88.

Liu Q, Tang Z, Surdenikova L, Kim S, Patel KN, Kim A*, et al.* (2009). Sensory neuron-specific GPCR Mrgprs are itch receptors mediating chloroquine-induced pruritus. Cell 139**:** 1353-1365.

Liu T, & Ji RR (2012). Oxidative stress induces itch via activation of transient receptor potential subtype ankyrin 1 in mice. Neurosci Bull 28**:** 145-154.

Mnyika KS, & Kihamia CM (1991). Chloroquine-induced pruritus: its impact on chloroquine utilization in malaria control in Dar es Salaam. J Trop Med Hyg 94**:** 27-31.

Motten AG, Martinez LJ, Holt N, Sik RH, Reszka K, Chignell CF*, et al.* (1999). Photophysical studies on antimalarial drugs. Photochem Photobiol 69**:** 282-287.

Palmaers NE, Wiegand SB, Herzog C, Echtermeyer FG, Eberhardt MJ, Leffler A (2021) Distinct Mechanisms Account for In Vitro Activation and Sensitization of TRPV1 by the Porphyrin Hemin. Int J Mol Sci. 22(19):10856

Ru F, Sun H, Jurcakova D, Herbstsomer RA, Meixong J, Dong X*, et al.* (2017). Mechanisms of pruritogen-induced activation of itch nerves in isolated mouse skin. J Physiol 595**:** 3651-3666.

Schmelz M (2021). How Do Neurons Signal Itch? Front Med (Lausanne) 8**:** 643006.

Shim WS, Tak MH, Lee MH, Kim M, Kim M, Koo JY*, et al.* (2007). TRPV1 mediates histamine-induced itching via the activation of phospholipase A2 and 12-lipoxygenase. J Neurosci 27**:** 2331-2337.

Taylor WR, & White NJ (2004). Antimalarial drug toxicity: a review. Drug Saf 27**:** 25-61.

Than JY, Li L, Hasan R, & Zhang X (2013). Excitation and modulation of TRPA1, TRPV1, and TRPM8 channel-expressing sensory neurons by the pruritogen chloroquine. J Biol Chem 288**:** 12818-12827.

Tsagareli MG, Nozadze I, Tsiklauri N, Carstens MI, Gurtskaia G, & Carstens E (2020). Thermal Hyperalgesia and Mechanical Allodynia Elicited by Histamine and Non-histaminergic Itch Mediators: Respective Involvement of TRPV1 and TRPA1. Neuroscience 449**:** 35-45.

Wilson SR, Gerhold KA, Bifolck-Fisher A, Liu Q, Patel KN, Dong X, *et al.* (2011). TRPA1 is required for histamine-independent, Mas-related G protein-coupled receptor-mediated itch. Nat Neurosci 14**:** 595-602.

Zhou FM, Cheng RX, Wang S, Huang Y, Gao YJ, Zhou Y*, et al.* (2017). Antioxidants Attenuate Acute and Chronic Itch: Peripheral and Central Mechanisms of Oxidative Stress in Pruritus. Neurosci Bull 33**:** 423-435.
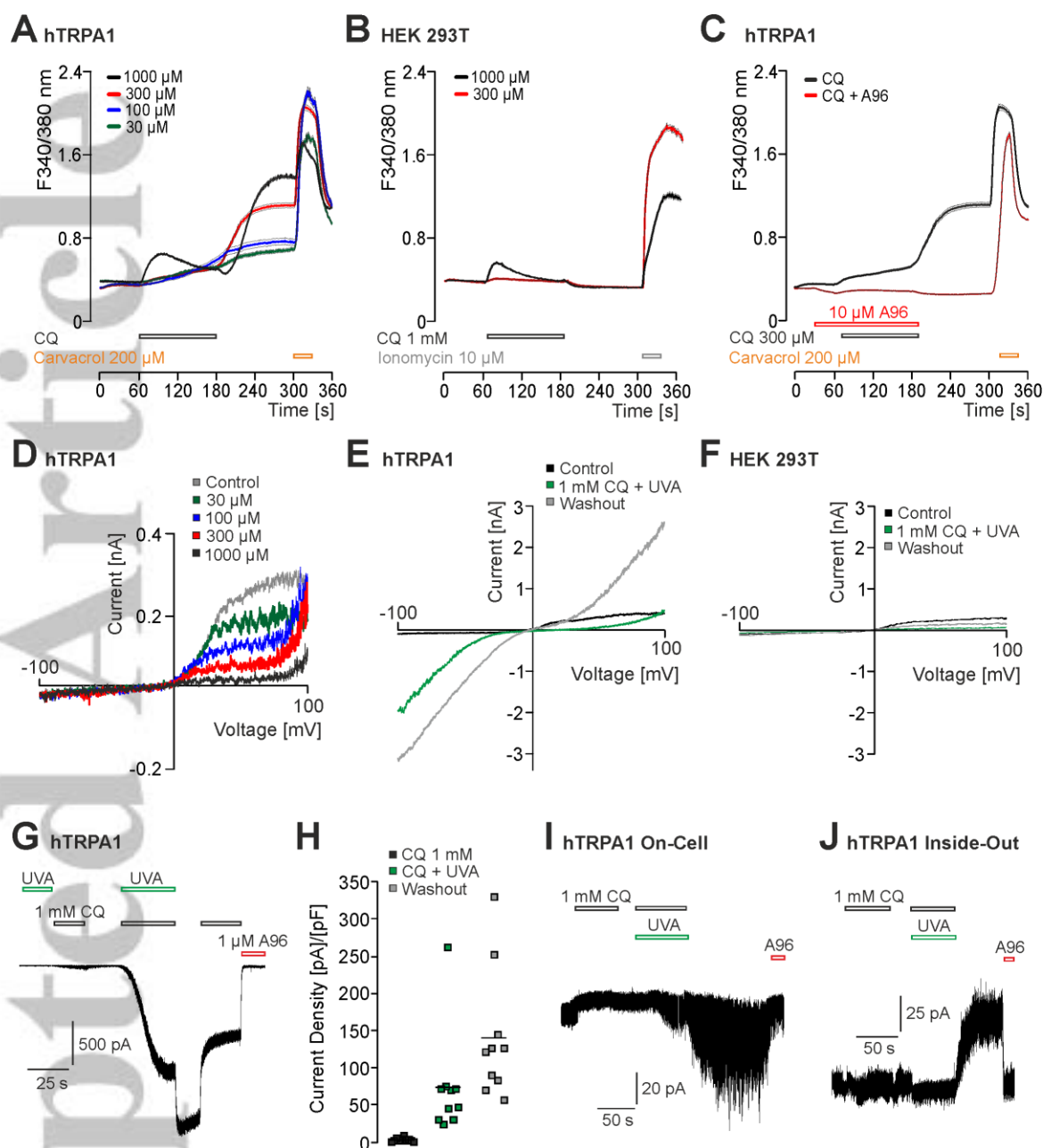
Figure 1. Chloroquine activates hTRPA1 when co-applied with UVA-light. A- C. Calcium-imaging on HEK 293 cells with or without expression of hTRPA1. A. In cells expressing hTRPA1, CQ induced a concentration-dependent increase in intracellular calcium (> 200 cells for each concentration). Note that the main increase in intracellular calcium developed following washout of CQ. B. In untransfected HEK 293t cells, 1 mM but not 300 μM CQ induced a small rapid increase in intracellular calcium (n= 282 and 461). No response was observed following washout of CQ. C. The CQ-induced (300 μM) calcium response in hTRPA1-expressing cells was effectively inhibited when the selective hTRPA1-inhibitor A967079 (10 μM) was co-applied with CQ (n= 546). In A- C, the average response is expressed as mean ± S.E.M. Carvacrol (200 μM) was applied at the end of experiment in order to identify cells expressing hTRPA1. D. Representative current trace of 500 ms long voltage ramps from -100 to +100 mV. hTRPA1-expressing cells generated outwardly

rectifying membrane currents which were inhibited by CQ in a concentration-dependent manner (n= 6). E. Typical example of an hTRPA1-expressing cell generating large membrane currents following simultaneous application of CQ and UVA-light 8(n= 8). Note that the current developed after CQ was washed out. F. Typical current traces on an untransfected HEK 293T cell treated with CQ and UVA-light (n= 6). G. Current trace showing an inward current induced by 1 mM CQ and UVA-light. Note the increase in current amplitude following washout of CQ and the concurrent inhibition by both CQ and A967079. The cell was held at - 60 mV. H. Current densities evoked by CQ, CQ + UVA-light and after washout of CQ (n= 10). I. Typical experiment performed in the on-cell mode displaying an A967079-sensitive membrane-current evoked by CQ applied together with UVA-light (n= 8). J. Representative cell-free inside-out recording displaying a membrane current evoked by co-application of CQ and UVA-light (n= 5). The holding potential was set at +60 mV.
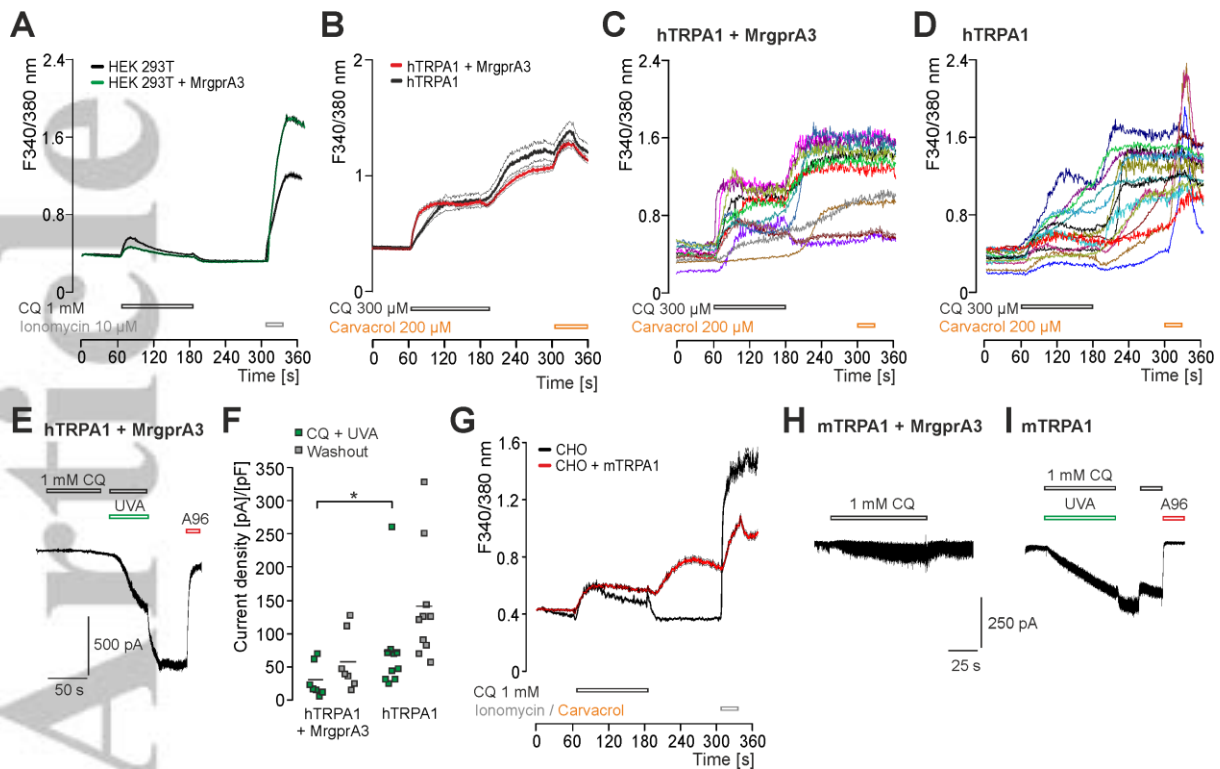
Figure 2. MrgprA3 is not required for activation of hTRPA1 by CQ and UVA-light.

A. Calcium-imaging on HEK 293T cells with or without expression of MrgprA3 (n= 889). Note that expression of MrgprA3 did not result in an increased response to 1 mM CQ. B- D. Calcium-imaging on hTRPA1-expressing HEK 293T cells with (n= 370) or without (n= 54) co-expression of MrgprA3. While the average responses are displayed in B, representative traces of individual cells are displayed in C and D. Calcium-influx induced by 300 μM CQ was similar in both cell types, but cells expressing MrgprA3 displayed responses with faster onset. E. Representative CQ + UVA-light induced inward current in a cell expressing both hTRPA1 and MrgprA3 (n= 7). The inward current resulting from washout of CQ was almost completely blocked by A967079. F. Current densities of CQ-induced inward currents in hTRPA1-expressing cells with and without MrgprA3. G. Calcium-imaging on CHO cells with (n= 476) or without (n= 296) expression of mTRPA1. The expression of mTRPA1 resulted in an increased response to 1 mM CQ. H. Representative whole-cell patch clamp trace

displaying the effect of 1 mM CQ on a CHO cell expressing mTRPA1 and MrgprA3 (n= 9). I. Typical patch clamp trace displaying the effect of 1 mM CQ + UVA-light on a CHO cell expressing mTRPA1 (n= 8).
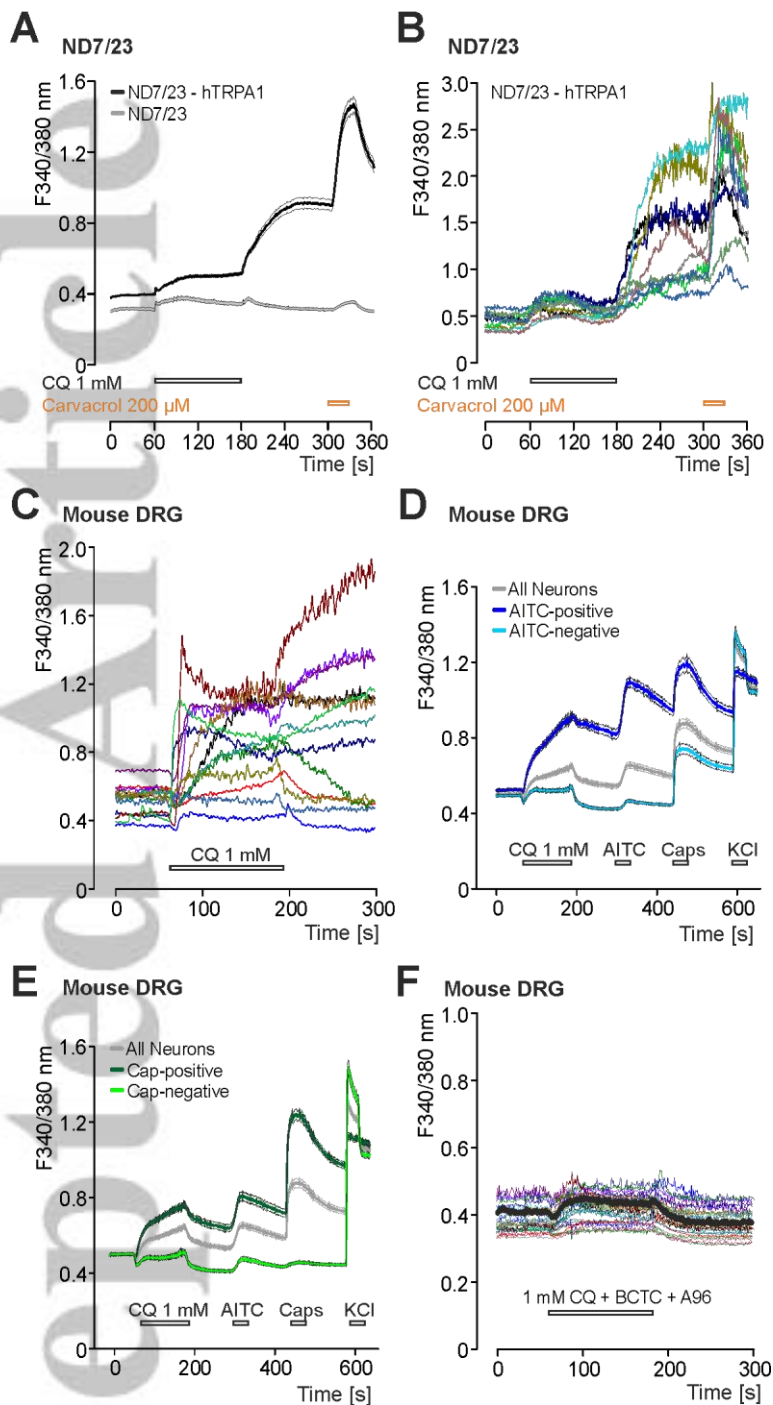
Figure 3. CQ-induced calcium-influx in ND7/23 cells and mouse DRG neurons.

A. Calcium-imaging on ND7/23 cells without (n= 354) and with (n= 373) transient expression of hTRPA1. Note that only cells expressing hTRPA1 displayed robust CQ-induced responses. B. Representative traces from individual cells in experiments explained for A. C. Calcium-imaging traces from individual mouse DRG neurons challenged with 1 mM CQ. Note that the shapes of CQ-induced responses are not

uniform. D. Mean calcium increase in mouse DRG neurons displayed as "all neurons" (grey, n= 459), "AITC-positive" (dark blue, n= 139) and AITC-negative (light blue, n= 320). All neurons were challenged with 1 mM CQ, 50 μm AITC, 100 nM capsaicin (Caps) and 40 mM KCl. E. Mean calcium increase in mouse DRG neurons displayed as "all neurons" (grey), "Cap-positive" (dark green, n= 236) and Cap-negative (light green, (n= 223). F. Representative traces from individual DRG cells as well as mean calcium increase (black line) in mouse DRG neurons evoked by 1 mM CQ in combination with A967079 and BCTC.
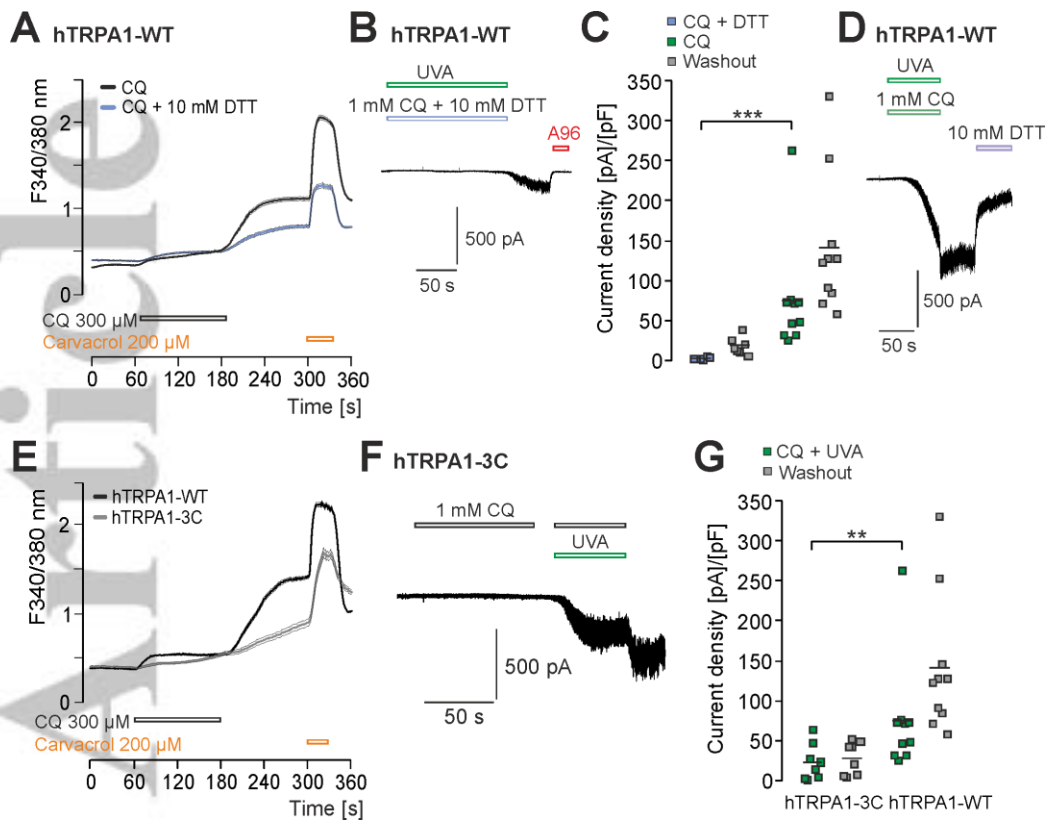
Figure 4. CQ-induced activation of hTRPA1 involves redox-sensitivity. A. Calcium-imaging on hTRPA1-expressing cells shows a decreased CQ-induced calcium response when CQ was co-applied with the reducing agent DTT (10 mM, blue line, n= 465). B. Original whole-cell patch clamp trace of hTRPA1 showing that CQ + UVA-light almost completely failed to evoke inward currents when DTT was co-applied (n= 7). C. Current densities of CQ-induced inward currents with and without 10 mM DTT. D. Typical current trace on hTRPA1-WT demonstrating that inward currents induced by CQ + UVA-light can be partly reversed by 10 mM DTT (n= 6). E. Calcium-imaging experiments performed with 300 µM CQ on hTRPA1-WT (black line) and the mutant hTRPA1-C621S/ C641S/C665S (hTRPA1-3C, gray line, n= 200). F. Whole-cell patch clamp recording on the hTRPA1-3C mutant displaying the effect of 1 mM CQ effect before and after illumination with UVA-light (n= 8). G. Current densities of CQ-induced inward currents on hTRPA1-WT and hTRPA1-3C.
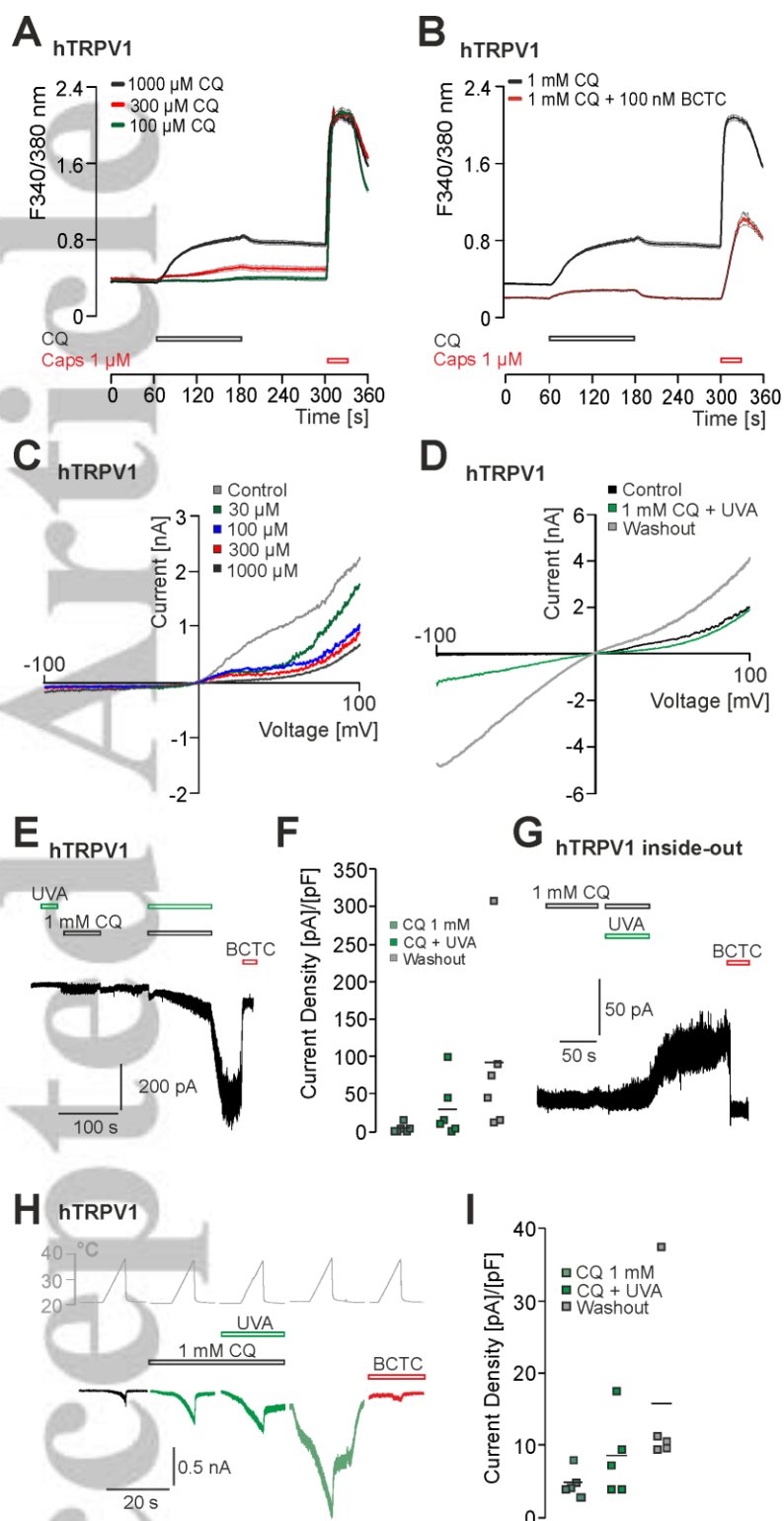
Figure 5. Chloroquine and UVA-light activate hTRPV1. A- B. Calcium-imaging on HEK 293 cells expressing hTRPV1 (n= 699). A. In cells expressing hTRPV1, CQ induced a concentration-dependent increase in intracellular calcium. Note that in contrast to hTRPA1, the main increase in intracellular calcium developed during

application of CQ. B. The CQ-induced (1 mM) calcium response in hTRPV1-expressing cells was effectively inhibited when the hTRPV1-inhibitor BCTC (100 nM) was co-applied with CQ (n= 117). In A and B, the average response is expressed as mean ± S.E.M. Capsaicin (Caps, 1 µM) was applied at the end of experiment in order to identify cells expressing hTRPV1. C and D. Representative current traces from hTRPV1-expressing cells. In C, CQ at increasing concentrations induced an inhibition of outward currents (n= 5). In D, CQ and UVA-light induced large membrane currents (n= 6). Note that the current developed after CQ was washed out. E. Current trace showing an inward current induced by 1 mM CQ and UVA-light on hTRPV1. Note the increase in current amplitude following washout of CQ and the inhibition by BCTC (n= 6). F. Current densities of currents evoked by CQ, CQ + UVA-light and after washout. G. Representative inside-out recording showing an activation of hTRPV1 upon application of CQ and UVA-light (n= 6). H. Representative current traces of heat-induced inward currents on hTRPV1. Application of 1 mM CQ induced a small potentiation of heat-evoked currents, this effect was increased by UVA-light (n= 7). I. Mean current densities evoked by heat without or with CQ or CQ + UVA-light.
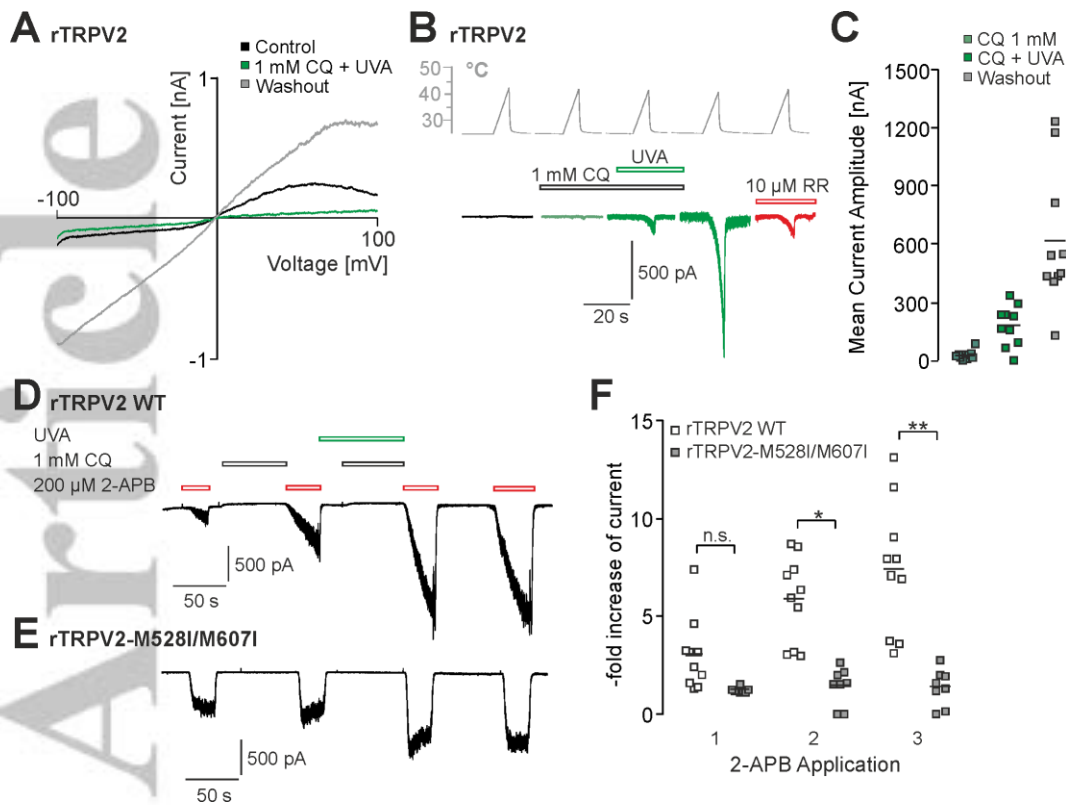
Figure 6. Chloroquine and UVA-light activate rTRPV2. A. Representative current trace from an rTRPV2-expressing cell generating large membrane currents following simultaneous application of CQ and UVA-light. Again, this current developed after CQ was washed out (n= 8). B. Representative current traces of heat-induced inward currents on rTRPV2. While application of 1 mM CQ failed to induce heat-evoked currents, CQ + UVA-light induced large heat-induced currents following washout of CQ (n= 10). These currents were blocked by ruthenium red (10 µM RR). C. Current densities evoked by heat without or with CQ or CQ + UVA-light. D, E. Current traces showing 2-APB-induced (200 µM) inward currents on rTRPV2-WT (D, n= 10) and the mutant rTRPV2-M528I/M607I (E, n= 8) before and during intermittent application of 1 mM CQ and UVA-light. F. Normalized CQ + UVA-light-induced increase of 2-APB-induced currents in D and E. Peak current amplitudes were normalized to the current evoked by the first application of 2-APB in each cell.
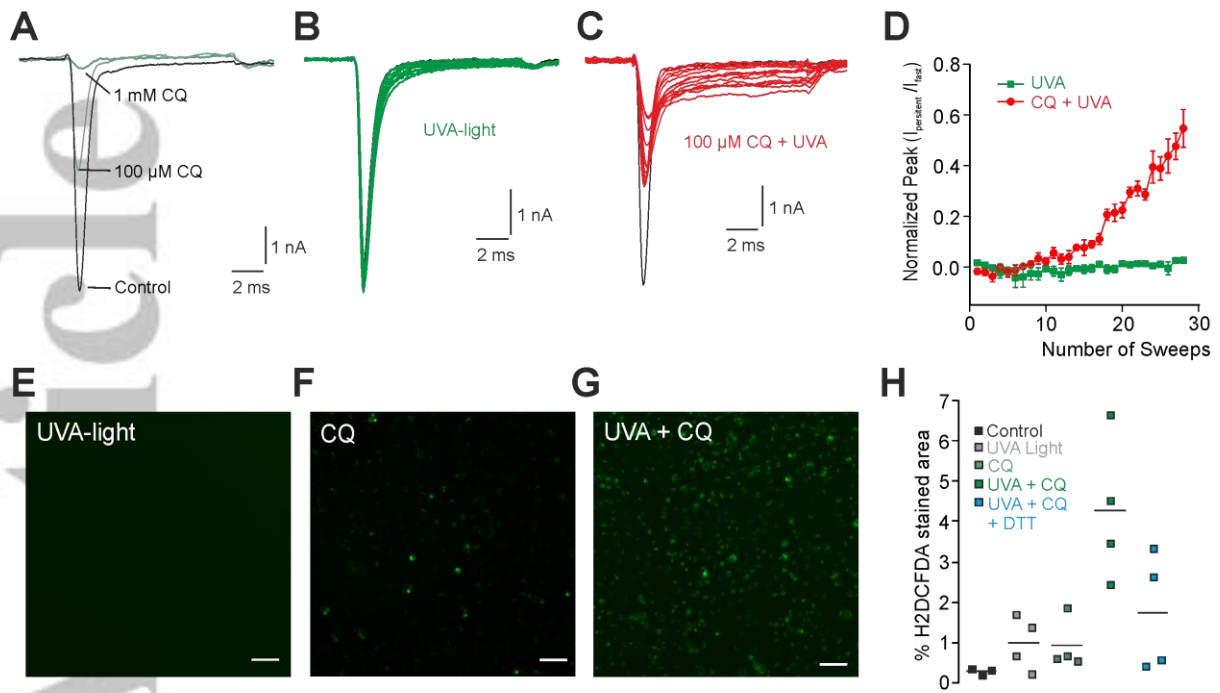
Figure 7. Chloroquine and UVA-light removes fast inactivation of voltage-gated sodium currents and induce an intracellular accumulation of ROS.

A- C. Representative currents traces generated by voltage-gated sodium channels endogenously expressed in ND7/23 cells. Cells were held at -120 mV and currents were evoked by 50 ms long pulses to 0 mV. A. Application of CQ alone resulted in a concentration-dependent block of sodium currents (n= 9). B. Illumination with UVA-light resulted in a modest removal of fast inactivation (n= 9). C. Co-application of CQ + UVA-light evoked a combined current inhibition and a strong removal of fast inactivation resulting in a large non-inactivating persistent current (n= 9). D. Amplitudes of the persistent current normalized with the peak current amplitude ($I_{persistent}/I_{fast}$) in cells treated with either UVA-light alone (green) or CQ + UVA-light (red). E- G. Images of ND7/23 cells stained with the ROS-indicator H2DCFDA. Cells were treated with UVA-light alone (E), with 300 µM CQ alone (F) or with CQ + UVA-light (G). H. Mean H2DCFDA-fluorescence intensities of cells from each treatment group (n= 4 for each group, ~45000 cells/experiment). Note that the reducing agent DTT induced a reduction of intracellular ROS in cells treated with CQ and UVA-light.
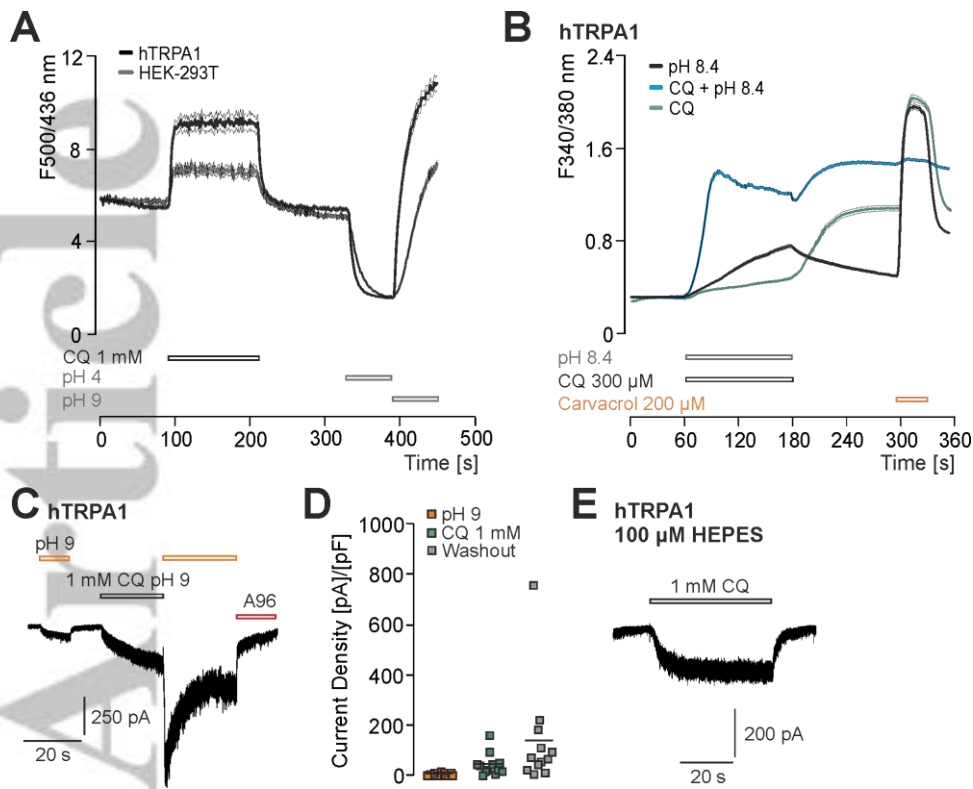
Figure 8. Chloroquine may activate hTRPA1 by inducing intracellular alkalosis.

A. BCECF-based ratiometric imaging on non-transfected (n= 537) and hTRPA1-expressing (n= 754) HEK 293 cells. In both cell lines, application of 1 mM CQ induced an instant and reversible increase in fluorescence ratio. This effect correlates with an intracellular alkalosis as was confirmed by application of control solution titrated to pH 4 or pH 9. B. Calcium-imaging experiments on hTRPA1-expressing cells treated with pH 8.4 (black, n= 883) alone, 300 µM CQ alone (green) 300 µM CQ at pH 8.4 (blue, n= 947). C. Representative whole-cell current trace on an hTRPA1-expressing cell treated with pH 9 and 1 mM CQ at pH 9 (n= 12). Note that UVA-light was not required for this CQ-induced activation of hTRPA1. D. Current densities of inward currents induced by pH 9 or 1 mM CQ + pH 9 and following washout of CQ at pH 9. E. Typical current trace generated by hTRPA1 upon application of 1 mM CQ in external solution with a reduced concentration of HEPES (100 µM, n= 8).
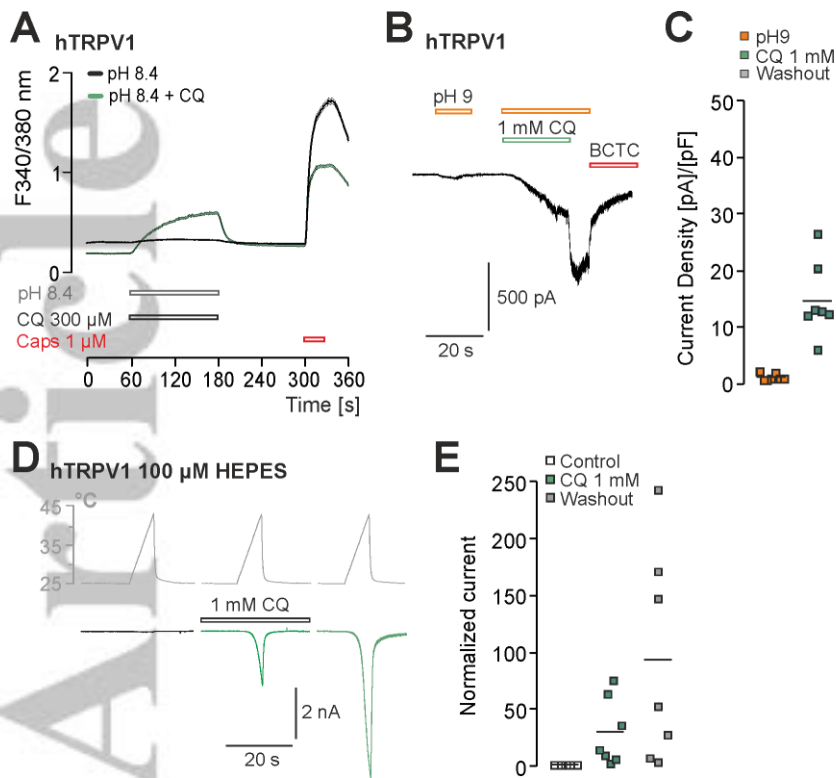
Figure 9. Alkalosis enhances UVA-light independent CQ-induced activation of hTRPV1. A. Calcium-imaging on hTRPV1-expressing cells treated with pH 8.4 (black, n= 495) alone or 300 µM CQ at pH 8.4 (green, n= 667). B. Whole-cell patch clamp recording on an hTRPV1-expressing cell treated with pH 9 and 1 mM CQ titrated to pH 9 (n= 7). C. Current densities of inward currents induced by pH 9 or 1 mM CQ + pH 9 and following washout of CQ at pH 9. D. Typical heat-induced currents generated by hTRPV1 upon application of 1 mM CQ in external solution with a reduced concentration of HEPES (100 µM, n= 8). E. Current densities of heat-induced currents induced by pH 9 or 1 mM CQ + pH 9 and following washout of CQ.